GA–A23312

DIII–D ADVANCED TOKAMAK RESEARCH OVERVIEW

by
V.S. CHAN, C.M. GREENFIELD, L.L. LAO, T.C. LUCE,
C.C. PETTY, G.M. STAEBLER, and the DIII–D TEAM

DECEMBER 1999

DISCLAIMER

GA–A23312

DIII–D ADVANCED TOKAMAK RESEARCH OVERVIEW

by
V.S. CHAN, C.M. GREENFIELD, L.L. LAO, T.C. LUCE,
C.C. PETTY, G.M. STAEBLER, and the DIII–D TEAM

This is a preprint of a paper presented at the Second IAEA Technical Committee Meeting on Steady State Operation of Magnetic Fusion Devices, October 25–29, 1999 in Fukuoka, Japan and to be published in *The Proceedings.*

Work supported by
the U.S. Department of Energy
under Contract Nos. DE-AC03-99ER54463, W-7405-ENG-48,
DE-AC05-96OR22464, DE-AC04-94AL85000, DE-AC02-76CH03073,
and Grant Nos. DE-FG03-86ER53225 and DE-FG03-95ER54294

GA PROJECT 30033
DECEMBER 1999

PAPER NO I–10

DIII–D ADVANCED TOKAMAK RESEARCH OVERVIEW

V.S. CHAN, C.M. GREENFIELD, L.L. LAO, T.C. LUCE, C.C. PETTY, G.M. STAEBLER, and the DIII–D Team

General Atomics, P.O. Box 85608, San Diego, California 92186-5608

Abstract

This paper reviews recent progress in the development of long-pulse, high performance discharges on the DIII–D tokamak. It is highlighted by a discharge achieving simultaneously β_NH of 9, bootstrap current fraction of 0.5, noninductive current fraction of 0.75, and sustained for 16 energy confinement times. The physics challenge has changed in the long-pulse regime. Non-ideal MHD modes are limiting the stability, fast ion driven modes may play a role in fast ion transport which limits the stored energy and plasma edge behavior can affect the global performance. New control tools are being developed to address these issues.

1. INTRODUCTION

The objective of the DIII–D Advanced Tokamak (AT) program is to establish a firm scientific basis for the optimization of the tokamak approach to fusion energy production. Since the beginning of the program about a decade ago, steady progress has been made in demonstrating improvements in stability, confinement, particle and heat-flux control, and noninductive current drive. The plan is to demonstrate these separately first and then simultaneously. This has produced solid scientific understanding which points the way to most promising directions for further improvements. To attain these improvements, new plasma control tools are being implemented. The goal of the new five-year program which began in 1999 is to simultaneously achieve high performance in β_N, confinement factor H and bootstrap current fraction f_{bs} in a regime relevant for the next step fusion device. The target is to achieve a β_NH product of 12, f_{bs} of greater than 0.5 and to sustain the high performance over 20 energy confinement times, τ_E.

Up until 1996, most of the DIII–D high performance discharges lasted for only a short duration. The challenge in research was to understand what caused the termination of the high performance. In 1996, initial results of high performance discharges were first reported [1] which lasted over several energy confinement times. Using the lower divertor pump for density control, a JET-shaped plasma with triangularity of 0.3 was sustained for over 2 seconds with a β_NH product of 7 although the bootstrap fraction of 0.3 was still relatively low. The plasma was characterized by benign edge localized modes (ELMs) at the H–mode edge which were recognized to beneficially control the edge pressure gradient. Further attempt to increase the performance by additional power led to the transition to large amplitude ELMs and beta saturation. It was speculated at the time that with the availability of the upper divertor pump (being installed at the time), capable of controlling the plasma density at high triangularity, better stability and hence higher performance should be expected.

2. HIGHLIGHT OF RECENT PROGRESS

Significant improvement of long-pulse AT performance has been achieved since 1996. Recent research has emphasized not only increasing the duration of high performance, but also increasing the fraction of bootstrap current. A summary of the progress in the development of high performance discharges on DIII–D is given by Fig. 1(a). High performance discharges include ELM-free H–modes which are usually short-lived, L–mode edge plasmas and ELMy H–mode plasmas which have longer durations. Indicated by large closed circles are representative key achievements in 1999, highlighted by an ELMing H–mode discharge with β_NH of 9 for 16 τ_E, a bootstrap fraction of 0.5, and a total non-inductive current fraction of 0.75 [2].This discharge is on the verge of reaching the next DIII–D research target which has been set with validating the performance of tokamak fusion reactor studies such as ARIES-RS [3] and SSTR [4] in mind. As shown in Fig. 1(b), the H factor of this particular discharge has reached the design value of ARIES-RS and SSTR. The β_N value reaches that of SSTR and is within 25% of ARIES-RS. This discharge has high triangularity of 0.7 and featured the favorable benign ELMs similar to the aforementioned 1996 discharge.

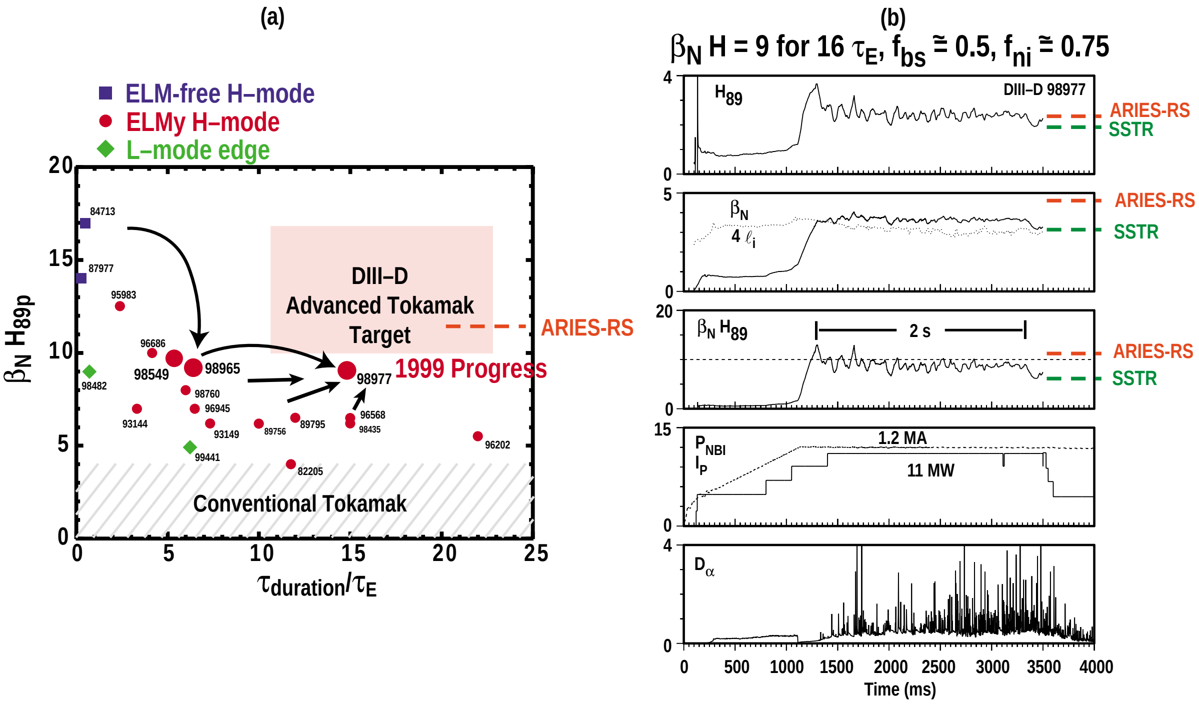

Fig. 1. Progress towards long-pulse, high performance operation on DIII–D.

The successful development of this discharge has benefited from understanding of the cause of termination of previous shorter duration discharges. Shown in Fig. 2 are three discharges with progressively longer duration of high performance. The short pulse, high performance plasma (dotted curve) was limited by ideal magnetohydrodynamic (MHD) instabilities as q_0 drops near 1 due to a strong core-edge coupling. Early beam injection (dashed curve) to raise q_{min} above 1 eliminated sawtooth and avoided the strong core-edge coupling. This resulted in a longer high performance duration. As the plasma rotation slowed down, the discharge suffered a beta collapse due to a non-ideal n=1 resistive wall mode (RWM). A small further increase in beam power was enough to sustain the plasma rotation and maintain stability against the non-ideal mode. This strategy has been successful in producing the majority of the long duration, high performance discharges in 1999.

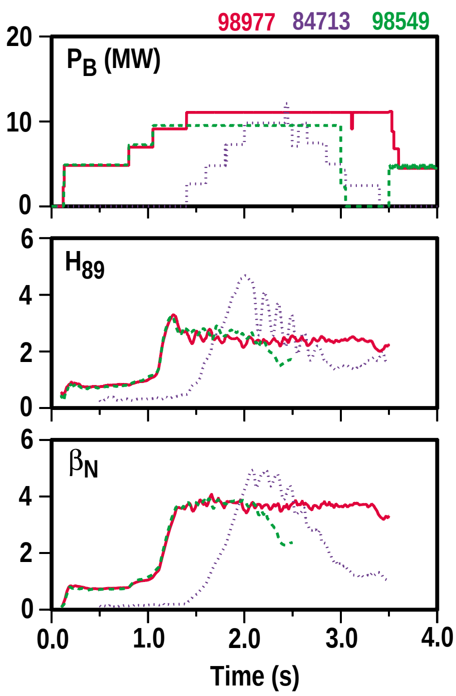

Fig. 2. Extension of high performance pulse duration using neutral beam timing control.

In assessing what has been learned from recent results, two new physics challenges have emerged which call for the development of better control tools. First, the β_N for a significant number of 1999 discharges is at or above the 4 l_i β limit — an empirical limit suggested from previous experiments. The 4 l_i limit can be traced back to an ideal MHD stability limit [5,6], It represents roughly the maximum no-wall β limit against the ideal n=1 mode. These new discharges are faced with a slower non-ideal instability limit. This is a new challenge for stability. Interestingly, the β_N value still seems to increase with l_i, which suggests that maintaining higher l_i should still be beneficial. Secondly, since the objective of the DIII–D AT research is not only to achieve high performance at long duration, but do it at a high bootstrap fraction, operation at high q_{min} (or equivalently high β_P) is required. Because neutral beam injection (NBI) was the primary heating tool available, and it has the tendency to drive central current, q_{min} continued to decrease during the discharges. As a result, the 1999 results fell short of achieving high performance at high q_{min} as intended. The situation calls for a better control of the current density profile. This will be possible when the off-axis electron cyclotron current drive (ECCD) system is available in the next campaign.

3. PHYSICS UNDERSTANDING

By performing detailed analyses on these long-pulse, high performance discharges, we have developed a deeper understanding of the causal effects on the formation and termination of the high performance phase. The transport properties are first discussed. In previous high performance ELM-free H–mode discharges, neoclassical ion thermal confinement was achieved across the entire plasma volume. This was accomplished through the establishment of overlapping edge and internal transport barriers. However, the transition to the ELMing phase was usually accompanied by some degradation in confinement [7]. Recent high performance long-pulse discharges [2] showed similar transport performance during the ELM-free phase, but unlike the older results, these recent discharges underwent a transition to the ELMing phase with little loss in performance as shown in Fig. 3.

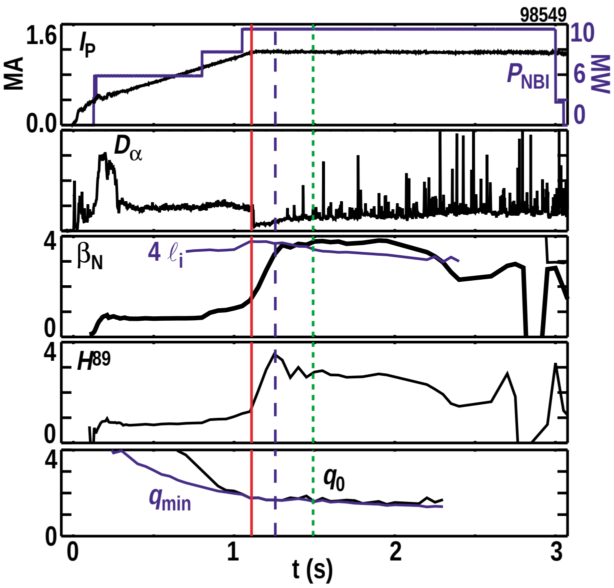

Fig. 3. A recent high performance ELMing H–mode discharge.

Analysis of the profiles in the L–mode, ELM-free H–mode and ELMing phase [indicated by solid, dashed, dotted lines, respectively in Fig. 4(a,b,c)] shows the following features. The formation of a transport barrier in the core began in the L–mode phase, which is especially evident in the T_i and rotation (Ω) profiles. In the ELM-free H–mode phase, the internal transport barrier (ITB) broadened considerably, at the same time, edge transport barrier appeared in the T_e and n_e profiles. Finally, in the ELMing phase, the ITB has significantly weakened due to the continual rise of the plasma density. The weakening of ITB with increasing density is consistent with previous observations.

In examining the thermal diffusivities [Fig. 5(a,b,c)], it is clear that even in the L–mode phase, the total ion diffusivity was already reduced to the Chang-Hinton neoclassical value $\left(\chi_i^{nc}\right)$ in the interior, confirming that an ITB was present. In the ELM-free phase, the combination of ITB and edge transport barrier helped to reduce χ_i to neoclassical level across the entire plasma, similar to what has been

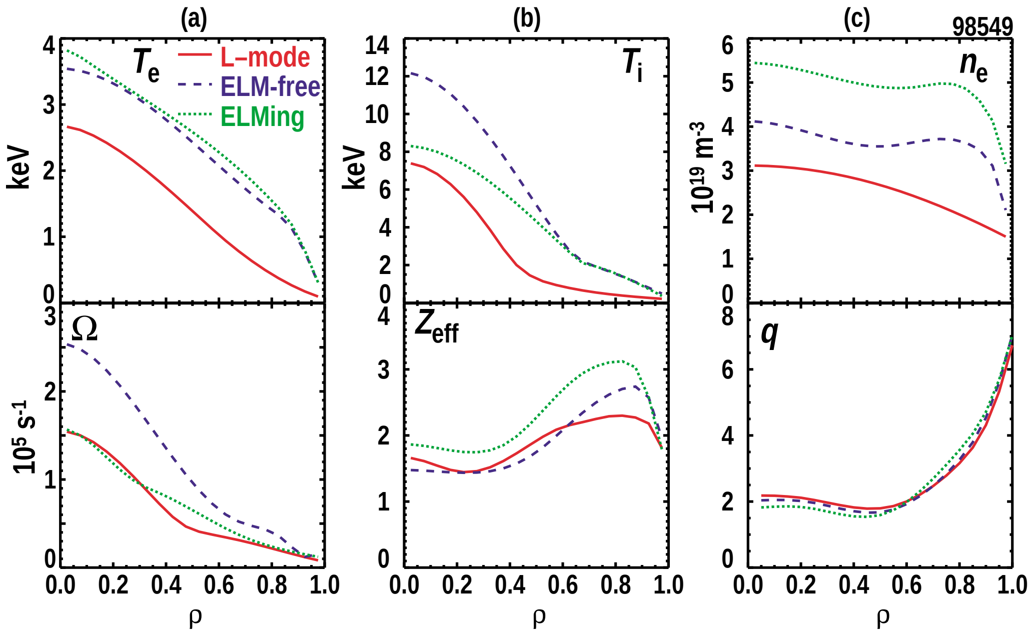

Fig. 4. Evolution of plasma profiles through L–mode, ELM-free and ELMing H–mode phase.

achieved previously. What is new and surprising is that in the ELMing phase, the ion transport increased only moderately throughout the plasma, remaining within roughly a factor of 2 of the neoclassical level over most of the plasma volume. This sequence of development suggests that with better density control, a strong ITB may be sustained even in the ELMing phase. During the whole discharge duration, the electron transport remained at L–mode level in the plasma interior, with some reduction seen in the H–mode edge region. Electron transport is an active research area [8] to explore for further confinement improvement.

From microstability analysis of the transport profiles using a gyrokinetic linear stability code [9], the paradigm of E×B shear suppression of ion temperature gradient (ITG) turbulence appears to correlate well with observation in the L–mode and ELM-free H–mode phase. Specifically, the calculated $\omega_{E\times B}$ shearing rate exceeded the maximum ITG growth rate, $\gamma_{max,}$ in the interior of the plasma which is where the ITB was observed in the L–mode phase [Fig. 6(a)] In the ELM-free H–mode phase, $\omega_{E\times B}$ exceeded γ_{max} over the entire volume [Fig. 6(b)] and ion neoclassical transport should be expected throughout. This has also been qualitatively observed. What remains to be explained is why the ion thermal transport increased by a factor of 2 in the ELMing phase even though the $\omega_{E\times B}$ was still much larger than the maximum growth rate [Fig. 6(c)]. One speculation is that although ion thermal transport may be solely governed by electrostatic turbulence like the ITG modes, fast ion transport could be significantly influenced by high frequency MHD activities which increase χ_i^{tot} as deduced from power balanced analysis. The observation of some MHD activities associated with these discharges, which will be discussed next, lends some credence to this view.

Turning our attention to stability, the focus is on what limits the high performance phase in recent discharges and the similarities and differences with pervious results. Previous high performance discharges typically terminated with the first appearance of a giant ELM, believed to be caused by low n-number ideal MHD modes [10]. Recent high performance discharges are robust to ELMs and low-n ideal modes. No significant ideal MHD activities were observed during the high performance phase and this is consistent with stability analysis showing that ideal n=1 kink mode is stable with the DIII–D conducting wall. The discharge is also stable to n=2 kink and high n ballooning modes. The cause of the beta rollover following a rapid rise (Fig. 7) appears to be correlated with the onset of Mirnov oscillations. At the time before the first ELM, some MHD signals appeared which are of particular interest. They are characterized by high frequency (~100 kHz) activities which are indicative of fast ion driven modes. These fast ion modes might be responsible for the enhanced fast ion transport that led to the beta rollover. More detailed study will be needed to confirm this.

The high performance phase usually ended with a beta collapse instead of a catastrophic crash. For the discharge shown in Fig. 7, the collapse was associated with a slowly rotating n=1 MHD mode. This mode has been identified as a RWM because of its slow growth rate, the real frequency matched the resistive wall time but not the fluid rotation speed, and it appeared above the no-wall ideal n=1

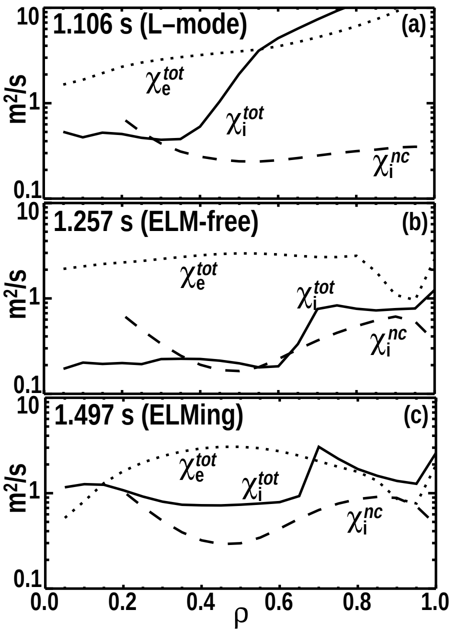

Fig. 5. Ion and electron thermal diffusivities during L–mode, ELM-free and ELMING H–mode.

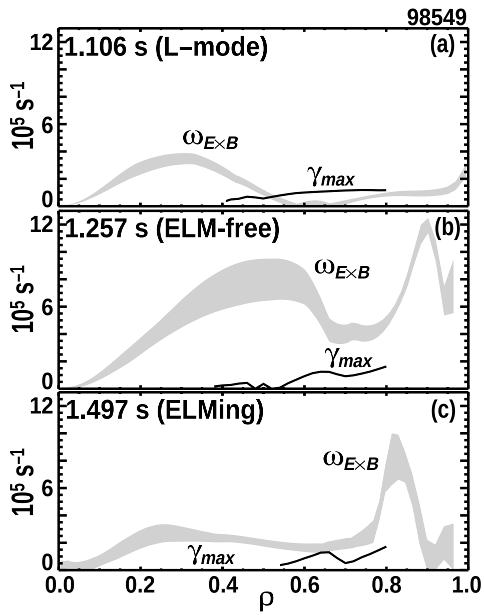

Fig. 6. Corresponding E×B shearing rate and maximum ITG growth rate.

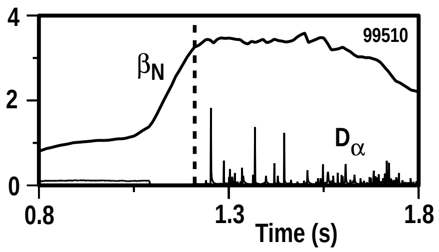

Fig. 7. Temporal behavior of stored energy of recent high performance ELMing H–mode.

limit ($\beta_N \gtrsim 4\ l_i$). The growth of the RWM leading to eventually the beta collapse is not well-understood. It could be that the RWM resonated with the static error fields which resulted in the slowing down of plasma rotation, further destabilizing the RWM due to a negative feedback. It should be possible to test such a theory by minimizing the static error fields. To prolong the stability to RWM, active feedback stabilization of RWM may be required. Feedback stabilization of RWM using external coils is an active research area in DIII–D.

Another non-ideal instability that sometimes terminated long-pulse discharges is the classical or neoclassical tearing mode [11]. However, tearing modes did not appear to play a role in these high performance long-pulse discharges. Tearing mode stability is apparently provided by the high shear at the outer rational surfaces because of lower edge current density. This appears to be consistent with the q-profiles of a discharge terminated by a 5/2 tearing mode and several stable high performance discharges. It is observed that the stable discharges have much stronger magnetic shear at the 5/2 rational surface. Tailoring the q-profile is thus an important technique to avoid tearing modes and for maintaining a large bootstrap fraction.

4. STRATEGY TO IMPROVE PERFORMANCE

Based on the scientific understanding, a strategy can be devised to further increase the duration of high performance as well as increasing the performance itself. It is recognized that sustaining the optimum q-profile and keeping q_{min} above 2 are important for both ideal and non-ideal MHD stability and for achieving high bootstrap current fraction. Analysis of the high performance phase of the long-pulse discharge yields the different current components. The NBI current peaks at the center as mentioned while the bootstrap current peaks at the edge leaving the ohmic current to fill the region half-way out to give the current profile for high stability. The ohmic current eventually relaxes resulting in an undesirable q-profile. Off axis-ECCD can be used to replace the ohmic component, thereby sustaining the optimum profile.

In DIII–D, localized off-axis ECCD has been demonstrated with two gyrotron sources [12]. The width of the measured electron cyclotron (EC) current profile as deduced from equilibrium reconstruction with Motional Stark Effect diagnostic is typically broader than the profile from theoretical ray-tracing calculation. Direct simulation of the MSE signals indicates that the actual ECCD may be narrower [13]. Linear ECCD theory is a lower bound to the present experimental data. At higher power, thus higher temperature, it should be possible to replace the off-axis ohmic current with ECCD using the gyrotron system which will be available in the 2000 campaign. We expect to have four gyrotrons routinely available for experiments providing up to 2.5 MW of absorbed power for heating and current drive.

It was mentioned earlier that the density rise was responsible for the weakening of the internal transport barrier. Keeping the density low and temperature high is also beneficial for current drive. The upper divertor pump with the 1999 configuration [Fig. 8(a)] has already demonstrated effectiveness in controlling the edge pedestal density, with up to 20% reduction. For the 2000 campaign, DIII–D will have additional pumping capability with a new baffled configuration [Fig. 8(b)]. Core density control should be more effective with this new system. Experimental time will be needed to develop effective use of the pump without exciting non-ideal MHD modes that were observed to cause transient decreases in beta.

To provide further control of RWM, an active feedback control system is being developed. The details of RWM studies on DIII–D have been reported elsewhere [14], suffice to report here that preliminary result from feedback using a saddle-coil configuration [Fig. 9(a)] has been quite encouraging. In this experiment [Fig. 9(b)], the RWM was destabilized when beta approached 4 ℓ_i. Without feedback, the RWM grew, was further enhanced by the slowing down of rotation, eventually caused the termination of the discharge. With feedback, the plasma recovered nicely from several MHD events, and was able to sustained a beta value at or above 4 ℓ_i for the duration of the feedback control. The feedback control system, in combination with q-profile control will eventually allow not only the extension of the high performance phase, but also higher beta values.

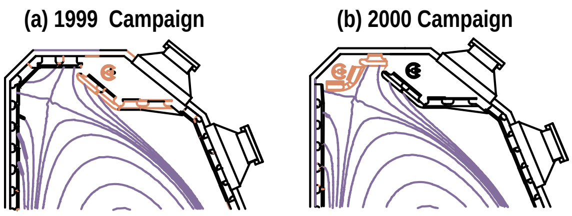

Fig. 8. Old and new upper divertor configuration.

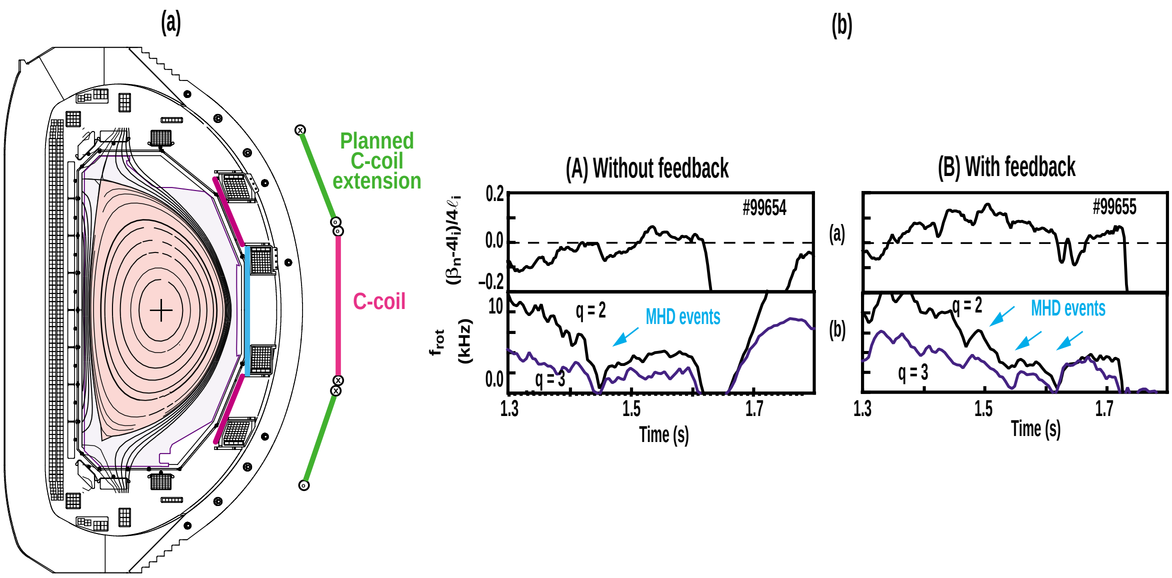

Fig. 9. Active feedback stabilization of RWMs.

Another important piece of the strategy is the maintenance and control of the ITB. In a scenario where NBI is involved, counter-NBI is promising for producing a broader internal transport barrier. This can be understood in terms of the differences in the $\omega_{E\times B}$ shearing profiles [15]. In the co-NBI discharges, the pressure gradient and rotation terms of the radial electric field equation (where κ_1 is of order one)

$$\frac{E_r}{RB_\theta} = \frac{V_\phi}{R} + \frac{1-\kappa_I}{Z_i e}\left(\frac{dT_i}{d\psi}\right) + \frac{T_i}{Z_i e n_i}\left(\frac{dn_i}{d\psi}\right) \ , \tag{1}$$

act to cancel at some radius leading to a narrow $\omega_{E\times B}$ profile concentrating near the core [Fig. 10(a)]. The same two terms are additive in the counter-NBI case resulting in a broader $\omega_{E\times B}$ shearing profile [Fig. 10(b)]. Again using the paradigm of E×B shear suppression of microturbulence [Fig. 11], one would expect a broader pressure profile that is also more favorable for MHD stability. By application of counter-NBI with good density control, there is a good chance to further improve both stability and confinement. This advantage has to be balanced against some cancellation of the non-inductive current because of the counter-NBI and the desirability of the resultant q-profile.

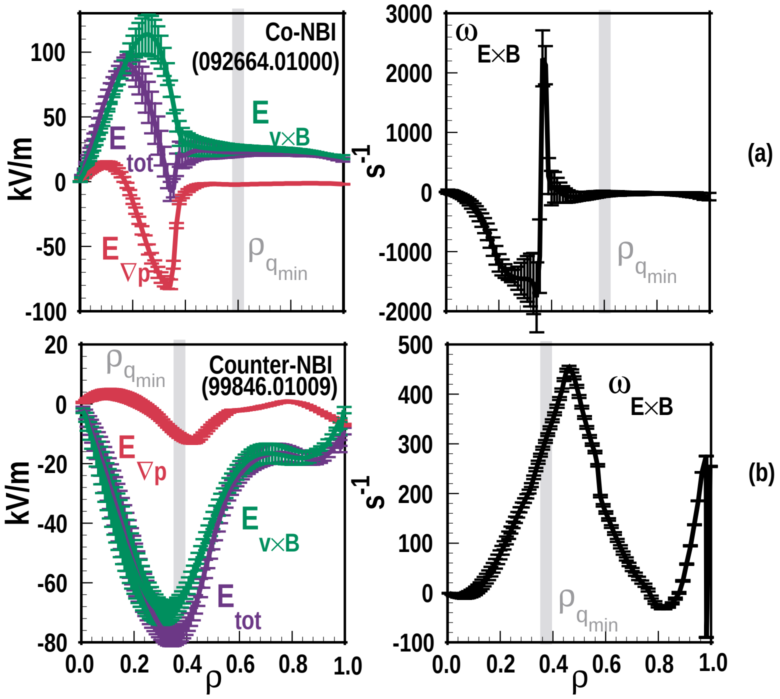

Fig. 10. E×B shearing profiles for co- and counter-NBI.

5. CONCLUDING REMARKS

DIII–D has recently concluded the first year of a five-year campaign with the goal of demonstrating the scientific viability of the long-pulse operation of high performance AT regime. Good progress has been made in establishing the physics basis for steady-state high performance operation. This is highlighted by achieving a $\beta_N H$ of 9, sustained for ~16 τ_E with f_{BS} ~ 0.5. The recent high performance discharges are characterized by ion thermal transport approaching two times neoclassical value during ELMing phase while electron transport remains at L–mode level. A β rollover limited the rapid increase in stored energy which may be caused by high frequency MHD modes driven by fast ions. The β collapse at the end of the high performance phase is due to non-ideal RWM destabilized when β_N exceeded the no-wall ideal n=1 limit. For further progress towards the five-year goal, off-axis ECCD is important to sustain high q_{min} and the current profile needed for stability. The new divertor configuration should provide more effective density control for good current drive efficiency and maintenance of ITB in ELMing phase. RWM eedback control and edge control will be used to stabilize both non-ideal modes and pressure driven edge modes which might be a limiting factor at higher beta. Finally, techniques such as counter-NBI will be exploited for controlling ITB in order to further enhance the confinement and stability.

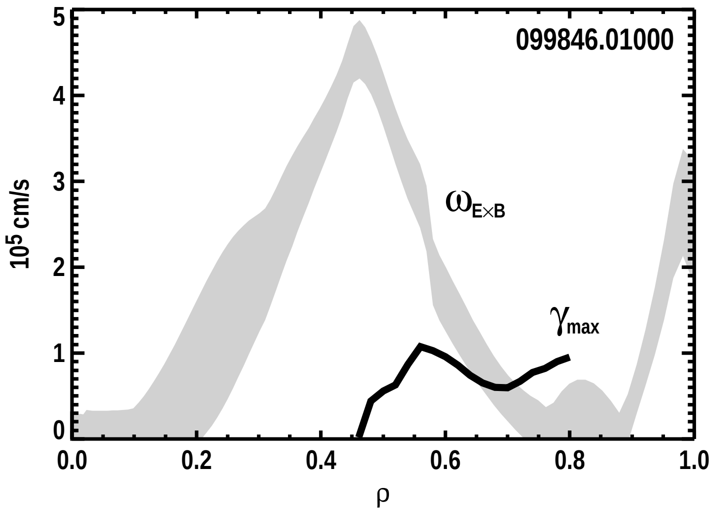

Fig. 11. E×B shear suppression of ITG turbulence up to ρ = 0.7 for counter-NBI.

Acknowledgment

This is a report of work supported by the U.S. Department of Energy under Contract Nos. DE-AC03-99ER54463, W-7405-ENG-48, DE-AC05-96OR22464, DE-AC04-94AL85000, DE-AC02-76CH03073, and Grant Nos. DE-FG03-86ER53225, and DE-FG03-95ER54294.

REFERENCES

[1] RICE, B.W., BURRELL, K.H., FERRON,J.R., GREENFIELD, C.M., JACKSON, G.L., LAO, L.L., LA HAYE, R.J., LUCE, T.C., et al., Nucl. Fusion **39**, 1855 (1999).

[2] GREENFIELD, C.M., et al., “Understanding and Control of Transport in Advanced Tokamak Regimes in DIII–D,” submitted to Phys. Plasmas.

[3] JARDIN, S.C., KESSEL, C.E., BATHKE, C.G., EHST, D.A., MAU, T.K., NAJMABADI, F., PETRIE, T.W., The ARIES Team, Fusion Eng. and Design **30**, 27 (1997).

[4] KIKUCHI, M., Nucl. Fusion **30**, 265 (1990).

[5] LAO, L.L., TAYLOR, T.S., CHU, M.S., CHAN, V.S., FERRON, J.R., STRAIT, E.J., Phys. Fluids **B4**, 232 (1992).

[6] HOWL, W., TURNBULL, A.D., TAYLOR, T.S., LAO, L.L., HELTON, F.J., FERRON, J.R., STRAIT, E.J., Phys. Plasmas **4**, 1724 (1992).

[7] LAZARUS, E.A., NAVRATIL, G.A., GREENFIELD, C.M., STRAIT, E.J., AUSTIN, M.E., BURRELL, K.H., CASPER, T.A., BAKER, D.R., et al., Phys. Rev. Lett. **77**, 2714 (1996).

[8] GREENFIELD, C.M., RETTIG, C.L., STAEBLER, G.M., STALLARD, B.W., AUSTIN, M.E., BURRELL, K.H., DeBOO, J.C. deGRASSIE, J.S., et al., Nucl. Fusion **39**, 1723 (1997).

[9] KOTSCHENREUTHER, M., REWOLDT, G., TANG, W.M., Comput. Phys. Commun. **88**, 128 (1995).

[10] STRAIT, E.J., CASPER, T.A., CHU, M.S., FERRON, J.R., GAROFALO, A.M., GREENFIELD, C.M., LA HAYE, R.J., LAO, L.L., et al., Phys. Plasmas **4**, 1783 (1997).

[11] LA HAYE, R.J., LAO, L.L., STRAIT, E.J., TAYLOR, T.S., Nucl. Fusion **37**, 397 (1997).

[12] LUCE, T.C., LIN-LIU, Y.R., HARVEY, R.W., GIRUZZI, G., POLITZER, P.A., RICE, B.W., LOHR, J.M., PETTY, C.C., PRATER, R., Phys. Rev. Lett. **83**, 4550 (1999).

[13] LUCE, T.C., PETTY, C.C., SCHUSTER, D.I., MAKOWSKI, M.A., “Determination of the Electron Cyclotron Current Drive Profile,” General Atomics Report GA–A23259 (1999).

[14] GAROFALO, A.M., TURNBULL, A.D., STRAIT, E.J., AUSTIN, M.E., BIALEK, J., CHU, M.S., FREDRICKSON, E., LA HAYE, R.J., et al., Phys. Plasmas **6**, 1893 (1999).

[15] STAEBLER, G.M., WALTZ, R.E., WILEY, J.C., Nucl. Fusion **37**, 287 (1997).